From Photons to Phonons and Back: A THz Optical Memory in Diamond

D. G. England, P. J. Bustard, J. Nunn, R. Lausten, and B. J. Sussman*

National Research Council of Canada, 100 Sussex Drive, Ottawa, Ontario K1A 0R6, Canada

(Received 23 August 2013; published 9 December 2013)

Optical quantum memories are vital for the scalability of future quantum technologies, enabling long-distance secure communication and local synchronization of quantum components. We demonstrate a THz-bandwidth memory for light using the optical phonon modes of a room temperature diamond. This large bandwidth makes the memory compatible with down-conversion-type photon sources. We demonstrate that four-wave mixing noise in this system is suppressed by material dispersion. The resulting noise floor is just 7×10^{-3} photons per pulse, which establishes that the memory is capable of storing single quanta. We investigate the principle sources of noise in this system and demonstrate that high material dispersion can be used to suppress four-wave mixing noise in Λ-type systems.

DOI: 10.1103/PhysRevLett.111.243601 PACS numbers: 42.50.Ex, 03.67.Hk, 03.67.Lx, 81.05.ug

Recent developments in the burgeoning field of quantum photonics have demonstrated that light is a promising carrier of quantum information [1]. Quantum-enhanced metrology [2], long-distance quantum communication [3], and photonic quantum processing [4,5] have been demonstrated using photons from pulsed parametric sources. Careful engineering has enabled the production of high-purity single photons [6–8] and exotic multiphoton states [9]. However, due to the probabilistic nature of most photon sources, multiphoton events are prohibitively rare, limiting these experiments to small (< 10) numbers of photons [10]. The development of high-fidelity quantum memories [11–13] offers a solution to this problem. For example, by storing multiple photons in an array of quantum memories and then releasing them all simultaneously, one could produce multiphoton states at dramatically increased rates [14]. These protocols place stringent requirements on memory performance, requiring the storage of high-bandwidth photons for many operational time bins.

Great progress has been made towards solid-state quantum memories, in particular, the storage of light in rare-earth ion doped solids [15,16] and electromagnetically induced transparency in optomechanical resonators [17,18]. However, such devices often require cryogenic cooling. Here, we demonstrate a THz-bandwidth memory for light in a room temperature solid-state system: the optical phonon modes of diamond. The capacity for quantum processing using diamond has previously been demonstrated by generating nonclassical correlations [19] and macroscopic entanglement [20]. Reference [19] exhibits an "emissive" quantum memory [21] in diamond; we build upon this result by demonstrating a full absorptive memory capable of storing and retrieving light at the single photon level.

Optical phonons are an attractive candidate for quantum storage as their high carrier frequency (40 THz [22]) permits broadband storage and suppresses thermal excitation at room temperature. Furthermore, the large electronic band gap in diamond [23] renders it transparent at all visible and near-infrared wavelengths, yielding the possibility for broadband operation over a wide range of carrier frequencies. These characteristics also make diamond an ideal candidate for interfacing with pulsed parametric photon sources, which are widely used in quantum photonics to produce high-quality single photons [6–8]. These sources are typically pumped by THz-bandwidth ultrafast lasers and, hence, are incompatible with optical memories that have MHz-GHz bandwidths.

Diamond is an ideal substrate in which to study the fundamental processes underpinning the memory interaction. In most systems employed for quantum memories, the quantum dynamics of the system are clouded by classical effects such as collisional dephasing, inhomogeneous broadening, or thermal noise. In contrast, at room temperature optical phonons in a high-purity single crystalline diamond are a near-pure quantum system containing a single optical phonon energy with a well-known quantum decay channel [24], a narrow linewidth compared to similar solids, and very little thermal phonon population. Hence, with no sample preparation, we have access to a pure quantum system with a simple level structure in which to investigate quantum dynamics, and capacity of diamond for high-fidelity single photon storage. Within this framework, the noise processes in the memory interaction are very well understood, allowing us to make detailed experimental and theoretical analyses. We show that the noise can be suppressed by material dispersion leading to a quantum-ready noise floor of just 7×10^{-3} photons per pulse.

In high-grade monocrystalline diamonds, the phonon population lifetime T_1 is dominated by the decay of the optical phonon into a pair of acoustic phonons via the Klemens channel [24–26]; typically in room temperature diamond this lifetime is $\sim$3.5 ps [19,27]. Previous measurements show that the ratio of the coherence lifetime T_2 to the phonon lifetime is $T_2/T_1 \approx 2$ [19], indicating that spectral diffusion and inhomogeneous broadening of the

optical phonon is small. We note that the T_1 lifetime could, in principle, be increased by careful engineering of a ^{12}C-^{13}C superlattice (as discussed in Ref. [19]), but this remains a significant technical challenge.

A memory lifetime of 3.5 ps is prohibitively short for use in a quantum repeater or for multiphoton engineering because the photon cannot be stored for long enough time to perform repeat-until-success strategies. Despite this short lifetime, a time-bandwidth product of 100 could be achieved if 30 fs pulses are stored. This time-bandwidth product should be sufficient to perform proof-of-principle quantum operations on a short time scale, making diamond a convenient ultrafast platform on which to explore simple quantum protocols.

To analyze the Raman interaction that underpins the memory, we model the memory as a Λ system consisting of the crystal ground state $|0\rangle$, an optical phonon acting as the storage state $|1\rangle$, and a far-off-resonant intermediate state $|2\rangle$ representing the conduction band [see Fig. 1(b)]. Input "signal" photons are written to, and read from, the memory using a Raman protocol [27,28] which has previously been used to demonstrate GHz-bandwidth storage in cesium vapor [13,29] and THz-bandwidth storage in hydrogen gas [30]. Writing and reading of the weak signal pulse is mediated by strong "read-write" pulses applied in

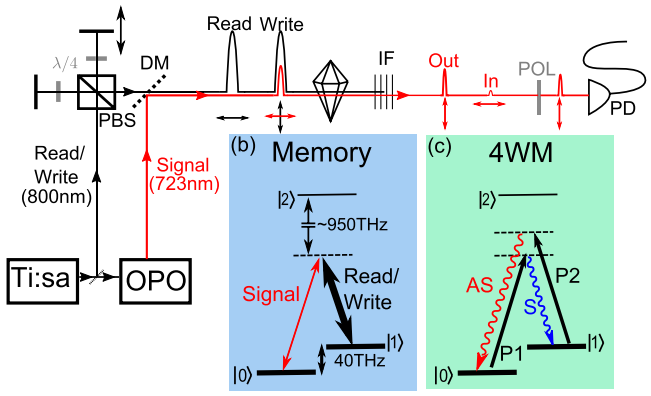

FIG. 1 (color online). (a) A Ti:sapphire oscillator (Ti:sa) at 800 nm is used to synchronously pump an OPO which creates the signal field at 723 nm. The remainder of the Ti:sapphire power provides the orthogonally polarized read-write pulses which are split, time delayed, and recombined on a polarizing beam splitter (PBS). Signal and read-write beams are overlapped on a dichroic mirror (DM) and focused into a diamond. After the diamond, interference filters (IF) remove the read-write beams and a polarizer (POL) selects the vertically polarized output mode which is detected on a photodiode (PD). (b) The memory states. The ground state $|0\rangle$ is coupled to the excited optical phonon band $|1\rangle$ by the signal and read-write beams which are in two-photon resonance with the phonon energy (40 THz). Both beams are far detuned from the conduction band $|2\rangle$. (c) The 4WM mechanism. Two pump photons $P1$ and $P2$ are scattered to produce Stokes (S) and anti-Stokes (AS) photons, respectively, [19].

2-photon Raman resonance with the excited optical phonon at 40 THz. In the write step, signal photons are annihilated in a Stokes transition and phonons are created. In the subsequent read step, phonons are annihilated in an anti-Stokes transition and signal photons are created [see Fig. 1(b)]. The Λ system also exhibits four-wave mixing (4WM) producing correlated pairs of Stokes and anti-Stokes photons [see Fig. 1(c)]. Four-wave mixing has previously been observed in diamond, providing evidence of nonclassical correlations and an emissive quantum memory [19]. In this work, however, 4WM is a source of undesirable noise photons.

The master laser for the experiment is a Ti:sapphire oscillator with a wavelength of $\lambda_{r/w} = 800$ nm (repetition rate 80 MHz, pulse energy 44 nJ, pulse duration 150 fs). Approximately half of the power is used to generate a write pulse and a time-delayed, orthogonally polarized read pulse ($\sim$10 nJ in each pulse). The remainder is used to synchronously pump an optical parametric oscillator (OPO) tuned to produce the signal pulses at $\lambda_s = 723$ nm (pulse energy $\simeq$ 1 pJ). The signal and read-write beams are combined on a dichroic mirror and focused into the diamond with the write and orthogonally polarized signal pulses temporally overlapped. Following the diamond, the signal beam is isolated using a series of interference filters and detected on a fast photodiode [see Fig. 1(a)].

We use a low-birefringence diamond of thickness 2.3 mm manufactured by Element Six Ltd. The diamond was grown by chemical vapor deposition and is cut along the $\langle 100\rangle$ face such that the Raman interaction couples fields of orthogonal polarization [31]. Hence, for maximum efficiency, the signal and write pulses are horizontally and vertically polarized, respectively. Readout of the stored coherence is performed using the horizontally polarized read pulse yielding a vertically polarized memory output. In this way, we can separate the input and output modes of the memory by their polarization.

We demonstrate the operation of our memory by scanning the read-write delay and measuring the memory output [see Fig. 2(a)]. At negative delays (read pulse before write), we see no signal in the vertically polarized output mode. A sharp step at zero delay indicates the onset of the memory interaction at which time the overall efficiency of the memory (storage and retrieval) is $\eta_{tot} \simeq 5\%$. The memory efficiency decreases exponentially with read-write delay, and the observed characteristic time scale of 3.5 ps is consistent with the T_1 decay time of the optical phonons [19]. With 10 nJ in both the read and the write pulse, we have a write efficiency of $\eta_{write} = 17\%$ and a maximum total efficiency of $\eta_{tot} = 5.3\%$. The read efficiency can be inferred as $\eta_{read} = \eta_{tot}/\eta_{write} = 31\%$.

The temporal evolution of the signal (anti-Stokes) field A, the Stokes field S, and the phonon amplitude Q in the presence of a strong pump (write-read) field are modeled according to the methods outlined in [32]. We remove any

dependence on the temporal shape of the write-read field by working with an effective dimensionless time coordinate ϵ that is proportional to the cumulative energy in the write-read pulse [28]. The resulting equations of motion are

$$\begin{aligned}[\partial_z - i\delta KL]A(\epsilon, z) &= iCQ(\epsilon, z),\\ \partial_z S^\dagger(\epsilon, z) &= -iCQ(\epsilon, z),\\ \partial_\epsilon Q(\epsilon, z) &= iC[A(\epsilon, z) + S^\dagger(\epsilon, z)],\end{aligned} \tag{1}$$

where z is the propagation distance as a fraction of the interaction length L within the diamond. Here, we have defined a dimensionless coupling constant C which parametrizes the strength of the Raman interaction and encompasses the contribution from both the material scattering cross section and the write-read pulse strength [13,28]. The phase mismatch arising from material dispersion is given by $\delta K = 2K_P - K_S - K_{AS}$, where $K_{P,S,AS}$ are the wave vectors of the pump, Stokes, and anti-Stokes fields in diamond.

To model the storage interaction, we treat A, S, Q as complex-valued functions and solve the system (1) with no input Stokes light or phonons and an anti-Stokes input of $A(\epsilon, 0) = A_{in}(\epsilon) = \sqrt{N_{in}}$. We have normalized the input so that $\int |A_{in}(\epsilon)|^2 d\epsilon = N_{in}$, with N_{in} the average number of input photons. Solving the equations provides us with a transmitted signal field, $A_{tr}(\epsilon) = A(\epsilon, 1)$, and a stored material excitation, $Q_{st}(z) = Q(1, z)$. The read interaction is then modeled by solving the equations a second time with the boundary conditions $Q(0, z) = e^{-\tau/2T_1} Q_{st}(z)$ and $S(\epsilon, 0) = A(\epsilon, 0) = 0$ to yield the memory output $A_{out}(\epsilon)$. Here τ is the delay between the read and write pulses. The interaction length can be approximated by the confocal parameter of the laser focus (480 μm), yielding $\delta KL = -5.05$ [33]. The power dependence of the write efficiency $\eta_{write} = 1 - \int |A_{tr}(\epsilon)|^2 d\epsilon / N_{in}$ [Fig. 2(c)] and the overall efficiency $\eta_{tot} = \int |A_{out}(\epsilon)|^2 d\epsilon / N_{in}$ [Fig. 2(b)] are fitted using this model to yield coupling parameters of $C_{write} = 0.44$ and $C_{read} = 0.58$ for the write and read interactions.

As a test of the coherence of the memory, we interfered, in free space, the retrieved output with a time-delayed replica of the input pulse; a first-order coherence of over 90% indicates that the memory interaction is highly coherent. This provides only a lower bound on the coherence of the memory process as the interference is degraded by imperfect spectral and temporal mode matching between the input and retrieved pulses in the interferometer. The coherence was measured as the storage time was increased and is plotted, alongside the memory efficiency, in Fig. 3. We see that the coherence remains constant around 90% despite an order of magnitude decrease in efficiency caused by the optical phonon decay. This confirms that while the magnitude of a stored state can be reduced by phonon decay, its coherence is unaffected—a key performance criterion for quantum memories [34–36].

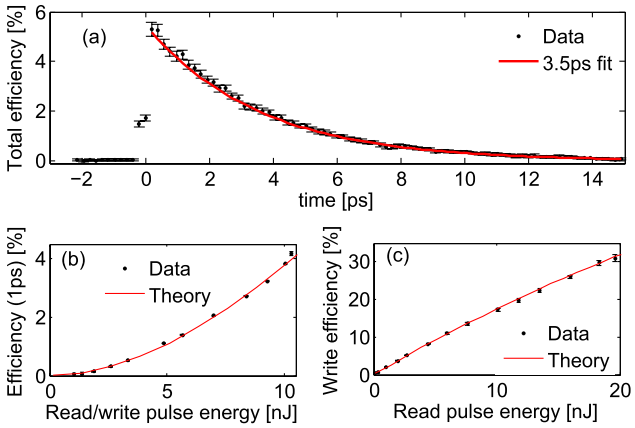

FIG. 2 (color online). (a) The total memory efficiency as a function of read-write delay (10 nJ each in read-write pulses). An exponential fit of 3.5 ps represents decay of the optical phonons into a pair of acoustic phonons. (b),(c) Total efficiency (at 1 ps storage time) and write efficiency, respectively, as a function of read-write pulse energy. The power dependence of the memory efficiencies is fitted by solving the system in Eq. (1).

The potential for quantum storage in the diamond memory was demonstrated by attenuating the input state such that, on average, $N_{in} = 0.6$ photons per pulse were incident on the diamond and the photodiode was replaced by a fiber-coupled avalanche photodiode to enable the detection of single photons. By blocking the input signal pulse, and applying only the read and write pulses, we measured the noise output of the memory to be, at most, 7×10^{-3} photons per pulse. We observe a high contrast between signal and noise [see Fig. 4(a)], offering a signal-to-noise ratio in excess of 7:1 when normalized to a single photon input.

Major sources of noise in memory systems include excited state fluorescence, spontaneous Raman scattering from thermal population of the storage state, and 4WM [37]. The conduction band in diamond is in the ultraviolet [23], so resonant fluorescence is irrelevant, and the diamond sample has very high purity, so fluorescence from

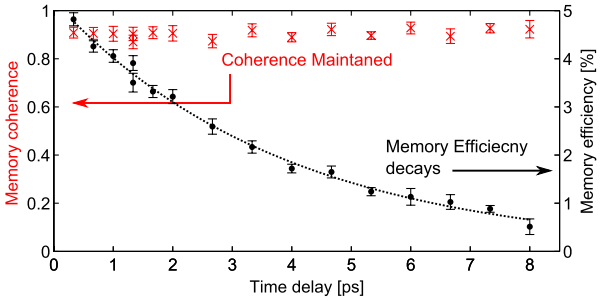

FIG. 3 (color online). The degree of first-order coherence between the memory output and a reference pulse (red crosses) remains high despite decaying memory efficiency (black dots). This confirms that the memory coherence is unaffected by decay of the optical phonon.

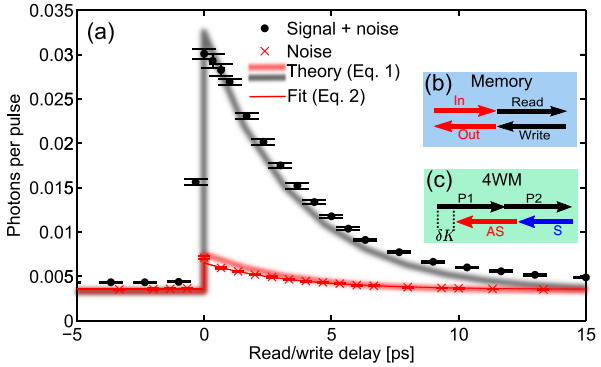

FIG. 4 (color online). (a) Memory output (black dots) with 0.6 photons per pulse at the input. With the input field blocked, the noise output is shown (red crosses) demonstrating good signal-to-noise contrast. The noise data are fitted with the phenomenological model outlined in Eq. (2) (thin solid red line). Thick transparent lines indicate the signal (black) and noise (red) measurements predicted by solving the coupled equations in Eq. (1). (b) Phase-matching diagram of the memory interaction showing perfect phase matching. (c) 4WM phase-matching diagram: A phase mismatch δK arises from the material dispersion and suppresses the 4WM process.

color centers is negligible [38]. The large phonon frequency ν_{ph} in diamond yields a thermal population of just $\mathcal{N}_{\mathrm{th}} = e^{-h\nu_{\mathrm{ph}}/k_B T} = 1.6 \times 10^{-3}$ phonons per mode at 25 °C. However, the 4WM observed in Ref. [19] is a significant source of noise in the memory.

The 4WM process is illustrated in Fig. 1(c). A pump photon from the read or write pulse ($P1$) is spontaneously scattered, producing a Stokes photon (S) and a phonon excitation. A second pump photon ($P2$) scatters from the phonon excitation to produce an orthogonally polarized anti-Stokes photon (AS). The S photons are removed by the interference filters, but the AS photons are the same wavelength and polarization as the signal photons and, hence, are a source of noise. Noise (AS) photons are polarized orthogonally to their parent photons, so a noise photon will only be detected if $P2$ is from the read pulse. However, the phonon can be produced by either the read or the write pulse. Phonons produced by the write pulse can decay before the read pulse arrives, leading to the delay dependence evident in Fig. 4(a).

We can write a phenomenological expression for the total number of noise photons $N_{\mathrm{noise}}(\tau)$ in terms of a time-dependent 4WM term and a constant thermal term:

$$N_{\mathrm{noise}}(\tau \geq 0) = \eta_{\mathrm{read}}[\mathcal{N}_{4\mathrm{WM}}(1 + e^{-\tau/T_1}) + \mathcal{N}_{\mathrm{th}}],$$
$$N_{\mathrm{noise}}(\tau < 0) = \eta_{\mathrm{read}}[\mathcal{N}_{4\mathrm{WM}} + \mathcal{N}_{\mathrm{th}}], \quad (2)$$

where $\mathcal{N}_{\mathrm{th}}$ and $\mathcal{N}_{4\mathrm{WM}}$ are the phonon populations per mode due to thermal excitation and 4WM, respectively. τ is the storage time, and T_1 is the phonon lifetime. We assume that the noise phonons are "readout" with the read efficiency of the memory η_{read}. The noise data in Fig. 4 are fitted by this model with T_1, $\mathcal{N}_{4\mathrm{WM}}$, and $\mathcal{N}_{\mathrm{th}}$ as free parameters. The resulting fit parameters are

$$\mathcal{N}_{4\mathrm{WM}} = 9.7 \times 10^{-3}, \quad \mathcal{N}_{\mathrm{th}} = 1.7 \times 10^{-3}, \quad T_1 = 3.4\ \mathrm{ps}. \quad (3)$$

A time of $T_1 = 3.4$ ps is characteristic of optical phonon decay in diamond (3.5 ps) and $\mathcal{N}_{\mathrm{th}}$ is consistent with Boltzmann statistics (1.6×10^{-3} at 25 °C); this shows that our simple model provides a faithful description of the noise process. The 4WM noise, which exceeds thermal noise by an order of magnitude at short delays, is the largest source of noise in the memory.

Material dispersion in the diamond leads to a phase mismatch δK in the 4WM process [see Fig. 4(c)], which explains the low efficiency observed in the emissive memory in Ref. [19]. In contrast the absorptive memory process is perfectly phase matched [Fig. 4(b)]. Hence, we can expect the 4WM noise to be suppressed relative to the memory process. The effect of this phase mismatch on the memory noise is investigated using the model described in Eq. (1). To predict the noise, Eq. (1) are solved as operator equations with a vacuum input signal $N_{\mathrm{in}} = 0$ [32]; both thermal and 4WM contributions to the noise output are included. The phase mismatch over the interaction region is given, as before, by $\delta KL = -5.05$. Using the coupling parameters $C_{\mathrm{read,write}}$ derived from the fits in Figs. 2(b) and 2(c), we calculate, from first principles, the signal and noise output of the memory; the theoretical photon counts are in excellent agreement with the measurements (diffuse lines in Fig. 4). Therefore, our model, which is based purely on the classical memory efficiency and the phase mismatch, accurately predicts the behavior of the memory at the quantum level.

These results indicate the crucial role that material dispersion plays in noise control: This feature is not unique to diamond; in fact, we expect it to be widely applicable to many Λ-type systems. Four-wave mixing noise suppression will be most effective in materials with high material dispersion and a large energy difference between the ground and storage states; such systems would provide not only high storage bandwidth, but also an in-built mechanism for suppressing noise. We also note that dispersion could be controlled, for example, using structured waveguides [39]. As an example, we use our model to calculate that a signal-to-noise ratio of over 100:1 could be achieved by increasing δKL to -19.

In conclusion, we have demonstrated a solid-state optical memory in diamond with the capability for quantum storage at room temperature. The memory has a bandwidth of 40 THz, making the diamond memory compatible with ubiquitous THz-bandwidth single photon sources. The diamond memory exhibits a coherence of over 90% and a quantum-ready noise floor of just 7×10^{-3} photons per pulse. Diamond is also an excellent candidate for etching microstructured photonic waveguides [40]. A diamond

memory could therefore be integrated into a compact photonic device. The noise floor is dominated by 4WM, which is a general problem in many Λ-type systems [13,37]. Here, we have demonstrated that this noise can be suppressed simply by material dispersion. These results show that high-bandwidth Raman-type optical memories offer both high-speed operation and an intrinsically low noise floor, and are well suited to the rigorous demands of quantum information processing.

The authors would like to thank Matthew Markham and Alastair Stacey of Element Six Ltd. for fabrication of the diamond sample. This work was supported by the Natural Sciences and Engineering Research Council of Canada.

*ben.sussman@nrc.ca

[1] H. J. Kimble, Nature (London) **453**, 1023 (2008).
[2] I. Afek, O. Ambar, and Y. Silberberg, Science **328**, 879 (2010).
[3] X.-S. Ma, T. Herbst, T. Scheidl, D. Wang, S. Kropatschek, W. Naylor, B. Wittmann, A. Mech, J. Kofler, E. Anisimova *et al.*, Nature (London) **489**, 269 (2012).
[4] M. A. Broome, A. Fedrizzi, S. Rahimi-Keshari, J. Dove, S. Aaronson, T. C. Ralph, and A. G. White, Science **339**, 794 (2013).
[5] J. B. Spring, B. J. Metcalf, P. C. Humphreys, W. S. Kolthammer, X.-M. Jin, M. Barbieri, A. Datta, N. Thomas-Peter, N. K. Langford, D. Kundys *et al.*, Science **339**, 798 (2013).
[6] P. J. Mosley, J. S. Lundeen, B. J. Smith, P. Wasylczyk, A. B. U'Ren, C. Silberhorn, and I. A. Walmsley, Phys. Rev. Lett. **100**, 133601 (2008).
[7] O. Cohen, J. S. Lundeen, B. J. Smith, G. Puentes, P. J. Mosley, and I. A. Walmsley, Phys. Rev. Lett. **102**, 123603 (2009).
[8] C. Söller, O. Cohen, B. J. Smith, I. A. Walmsley, and C. Silberhorn, Phys. Rev. A **83**, 031806 (2011).
[9] C.-Y. Lu, X.-Q. Zhou, O. Guhne, W.-B. Gao, J. Zhang, Z.-S. Yuan, A. Goebel, T. Yang, and J.-W. Pan, Nat. Phys. **3**, 91 (2007).
[10] X.-C. Yao, T.-X. Wang, P. Xu, H. Lu, G.-S. Pan, X.-H. Bao, C.-Z. Peng, C.-Y. Lu, Y.-A. Chen, and J.-W. Pan, arXiv:1105.6318.
[11] H. Zhang, X.-M. Jin, J. Yang, H.-N. Dai, S.-J. Yang, T.-M. Zhao, J. Rui, Y. He, X. Jiang, F. Yang *et al.*, Nat. Photonics **5**, 628 (2011).
[12] H. P. Specht, C. Nolleke, A. Reiserer, M. Uphoff, E. Figueroa, S. Ritter, and G. Rempe, Nature (London) **473**, 190 (2011).
[13] K. F. Reim, P. Michelberger, K. C. Lee, J. Nunn, N. K. Langford, and I. A. Walmsley, Phys. Rev. Lett. **107**, 053603 (2011).
[14] J. Nunn, N. K. Langford, W. S. Kolthammer, T. F. M. Champion, M. R. Sprague, P. S. Michelberger, X.-M. Jin, D. G. England, and I. A. Walmsley, Phys. Rev. Lett. **110**, 133601 (2013).
[15] C. Clausen, F. Bussières, M. Afzelius, and N. Gisin, Phys. Rev. Lett. **108**, 190503 (2012).
[16] E. Saglamyurek, N. Sinclair, J. Jin, J. A. Slater, D. Oblak, F. Bussieres, M. George, R. Ricken, W. Sohler, and W. Tittel, Nature (London) **469**, 512 (2011).
[17] A. H. Safavi-Naeini, T. P. M. Alegre, J. Chan, M. Eichenfield, M. Winger, Q. Lin, J. T. Hill, D. E. Chang, and O. Painter, Nature (London) **472**, 69 (2011).
[18] S. Weis, R. Rivire, S. Delglise, E. Gavartin, O. Arcizet, A. Schliesser, and T. J. Kippenberg, Science **330**, 1520 (2010).
[19] K. Lee, B. Sussman, M. Sprague, P. Michelberger, K. Reim, J. Nunn, N. Langford, P. Bustard, D. Jaksch, and I. Walmsley, Nat. Photonics **6**, 41 (2012).
[20] K. C. Lee, M. R. Sprague, B. J. Sussman, J. Nunn, N. K. Langford, X.-M. Jin, T. Champion, P. Michelberger, K. F. Reim, D. England *et al.*, Science **334**, 1253 (2011).
[21] L.-M. Duan, M. D. Lukin, J. I. Cirac, and P. Zoller, Nature (London) **414**, 413 (2001).
[22] S. A. Solin and A. K. Ramdas, Phys. Rev. B **1**, 1687 (1970).
[23] C. D. Clark, P. J. Dean, and P. V. Harris, Proc. R. Soc. A **277**, 312 (1964).
[24] P. G. Klemens, Phys. Rev. **148**, 845 (1966).
[25] M. S. Liu, L. A. Bursill, S. Prawer, and R. Beserman, Phys. Rev. B **61**, 3391 (2000).
[26] F. C. Waldermann, B. J. Sussman, J. Nunn, V. O. Lorenz, K. C. Lee, K. Surmacz, K. H. Lee, D. Jaksch, I. A. Walmsley, P. Spizziri *et al.*, Phys. Rev. B **78**, 155201 (2008).
[27] A. E. Kozhekin, K. Mølmer, and E. Polzik, Phys. Rev. A **62**, 033809 (2000).
[28] J. Nunn, I. A. Walmsley, M. G. Raymer, K. Surmacz, F. C. Waldermann, Z. Wang, and D. Jaksch, Phys. Rev. A **75**, 011401 (2007).
[29] K. Reim, J. Nunn, V. Lorenz, B. Sussman, K. Lee, N. Langford, D. Jaksch, and I. Walmsley, Nat. Photonics **4**, 218 (2010).
[30] P. J. Bustard, R. Lausten, D. G. England, and B. J. Sussman, Phys. Rev. Lett. **111**, 083901 (2013).
[31] W. Hayes and R. Loudon, *Scattering of Light by Crystals* (Dover Science, New York, 1978).
[32] C. Wu, M. G. Raymer, Y. Y. Wang, and F. Benabid, Phys. Rev. A **82**, 053834 (2010).
[33] *Handbook of Optical Constants of Solids*, edited by E. D. Palik (Elsevier, New York, 1997).
[34] Y.-W. Cho and Y.-H. Kim, Opt. Express **18**, 25 786 (2010).
[35] D. G. England, P. S. Michelberger, T. F. M. Champion, K. F. Reim, K. C. Lee, M. R. Sprague, X.-M. Jin, N. K. Langford, W. S. Kolthammer, J. Nunn *et al.*, J. Phys. B **45**, 124008 (2012).
[36] M. U. Staudt, S. R. Hastings-Simon, M. Nilsson, M. Afzelius, V. Scarani, R. Ricken, H. Suche, W. Sohler, W. Tittel, and N. Gisin, Phys. Rev. Lett. **98**, 113601 (2007).
[37] N. Lauk, C. O'Brien, and M. Fleischhauer, Phys. Rev. A **88**, 013823 (2013).
[38] S. Pezzagna, D. Rogalla, D. Wildanger, J. Meijer, and A. Zaitsev, New J. Phys. **13**, 035024 (2011).
[39] A. D. Falco, L. O'Faolain, and T. F. Krauss, Appl. Phys. Lett. **92**, 083501 (2008).
[40] M. P. Hiscocks, K. Ganesan, B. C. Gibson, S. T. Huntington, F. Ladouceur, and S. Prawer, Opt. Express **16**, 19 512 (2008).